Appendix X. Ocean Ecosystems Sensitivity Analyses and Measurement Requirements

The appendix has four sections on remotely sensed optical, biological, and biogeochemical parameters related to the science questions, atmospheric correction sensitivity to noise, bio-optical algorithm sensitivity to noise, and a summary of ocean radiometer measurement requirements. The atmospheric correction analysis was conducted by Menghua Wang (NOAA/NESDIS) and Howard Gordon (U. of Miami). The bio-optical algorithm study was conducted by Stephane Maritorena (UC/Santa Barbara) using inputs from the Wang and Gordon study.

Remotely Sensed Ocean Optical, Biological, and Biogeochemical Parameters

Associated with each of the science questions is a set of bio-optical parameters that must be measured in order to address the question. Each parameter requires an algorithm which transforms the basic water-leaving radiances or remote sensing reflectances into an estimated value of that parameter over a range of values. Table 1 provides the list of parameters and the range of values commonly observed in marine and estuarine waters. The range of values that can be estimated from satellite radiometry depends on the spectral bands and data quality of the sensor (e.g., signal-to-noise ratio and radiometric accuracy) and the sensitivity of the algorithms.

Table 1. Remotely sensed optical and biogeochemical parameters with the range of values commonly observed in the ocean and coastal estuaries.

Simulations for the NIR and SWIR SNR Requirements for Atmospheric Corrections

Atmospheric correction for ocean color product is extremely sensitive to sensor spectral band calibration errors, as well as to radiometric noise. This is due to the considerably low radiance from the ocean compared to the sensor-measured top-of-atmosphere (TOA) radiance. The sensor spectral band radiometric performance can be characterized by the signal to noise ratio (SNR). To understand the radiometric noise effects on the derived normalized water-leaving reflectance spectra, simulations of atmospheric correction, using the two near-infrared (NIR) bands (765 and 865 nm) and various combinations of the shortwave infrared (SWIR) bands (1240, 1640, and 2130 nm), have been carried out for several levels of sensor noise.

Noise Model. A Gaussian distribution (with mean value = 0) is used for the noise simulations. The standard deviation (STD) of the Gaussian distribution is the radiance noise level (i.e., related to the SNR values). The simulated reflectance noise is then added into the TOA reflectance at various NIR and SWIR bands that are used for making atmospheric correction. Eight noise levels are generated, corresponding to eight SNR values of 25, 50, 100, 200, 400, 600, 800, and 1000. It is noted that the reflectance noise is only added into the bands that are used for atmospheric correction (e.g., two NIR bands), and UV and visible bands are noise free in all simulations discussed in this subsection. The reflectance noises are spectrally incoherent.

Atmospheric Correction. Atmospheric correction simulations using two NIR bands (Gordon and Wang, 1994) and various SWIR bands (Wang, 2007) have been carried out including reflectance noise levels for the corresponding NIR and SWIR bands. Specifically, simulations were carried out for a typical Maritime aerosol model (M80) and a Tropospheric model (T80), where the T80 model is actually M80 model without the large size fraction, for aerosol optical

thicknesses (at 865 nm) of 0.05, 0.1, 0.2, and 0.3. The M80 and T80 aerosol models were not used in the aerosol lookup tables for atmospheric correction (Gordon and Wang, 1994; Wang, 2007). Simulations were performed for a case with solar-zenith angle of 60°, sensor-zenith angle of 45°, and relative azimuth angle of 90°.

SNR Simulations. For each case, atmospheric correction for 5000 noise realizations with a given SNR value was carried out. For example, for a case with aerosol optical thickness (AOT) at 865 nm of 0.1, 5000 reflectance noise samples (with a given SNR value) were generated and added into the TOA NIR (765 and 865 nm) reflectance values. The NIR atmospheric correction (Gordon and Wang, 1994) was then performed 5000 times to generate the corresponding normalized water-leaving reflectance spectra error. The same procedure was carried out for all four AOTs and also for the SWIR algorithm (Wang, 2007). In the SWIR atmospheric correction, however, the Gaussian noise was of course added into the SWIR bands (error free for UV to NIR bands). This produces the uncertainty in the derived normalized water-leaving reflectance from the UV to the red (or NIR in the case of the SWIR bands). In effect, the simulated uncertainty includes errors from both the atmospheric correction algorithm and the added Gaussian noise in the NIR or SWIR bands. The reflectance uncertainty spectra (from UV to red) are then used for the bio-optical model sensitivity analysis by Stephane Maritorena.

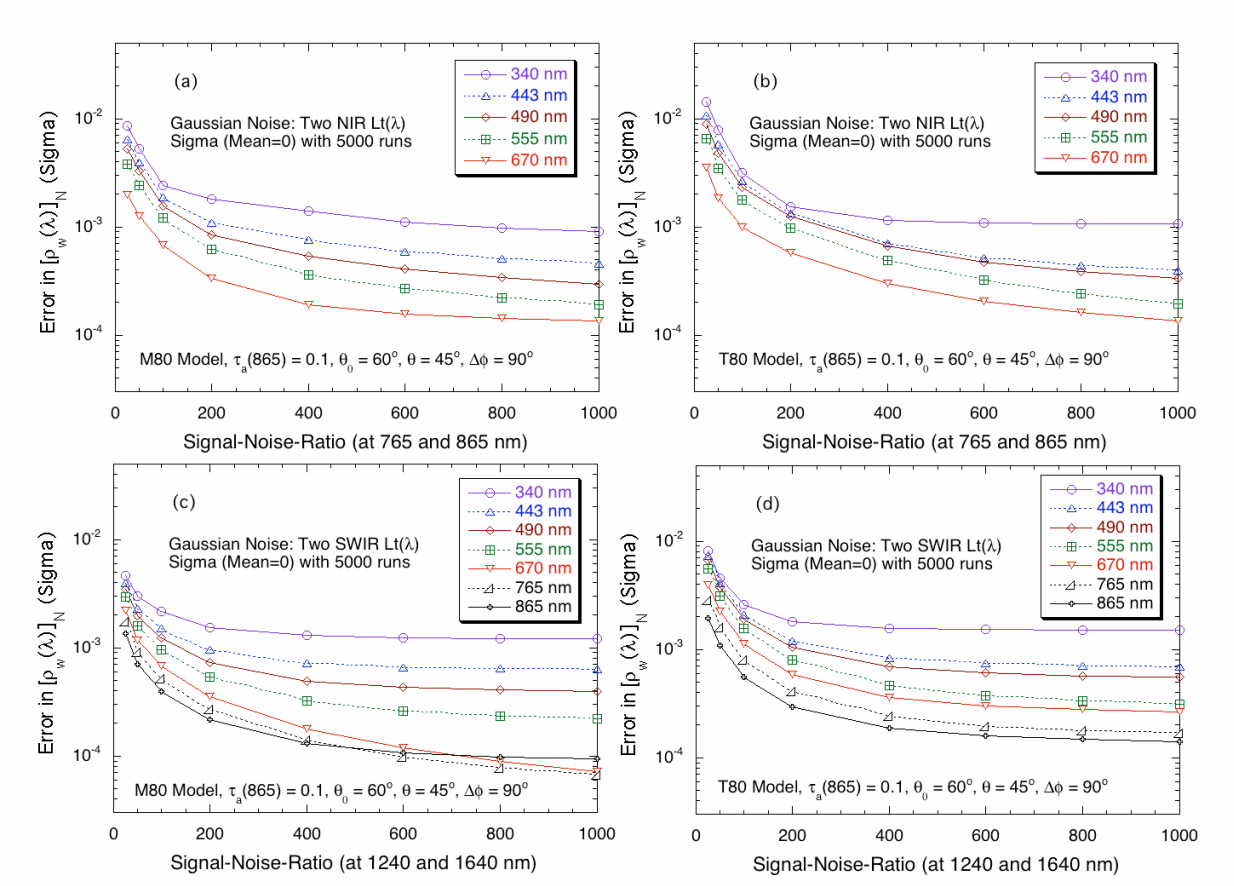

Figure 1. Error in the derived normalized water-leaving reflectance (in standard deviation with the mean value of 0) from 5000 Gaussian noise realizations as a function of the SNR value using the NIR (plots a and b) and SWIR (plots c and d) atmospheric correction algorithms. Aerosol model and AOT value, as well as solar-sensor geometry are indicated in each plot. For the NIR algorithm, error spectra data from UV to red are provided (plots a and b), while for the SWIR algorithm error spectra from UV to NIR are shown (plots c and d).

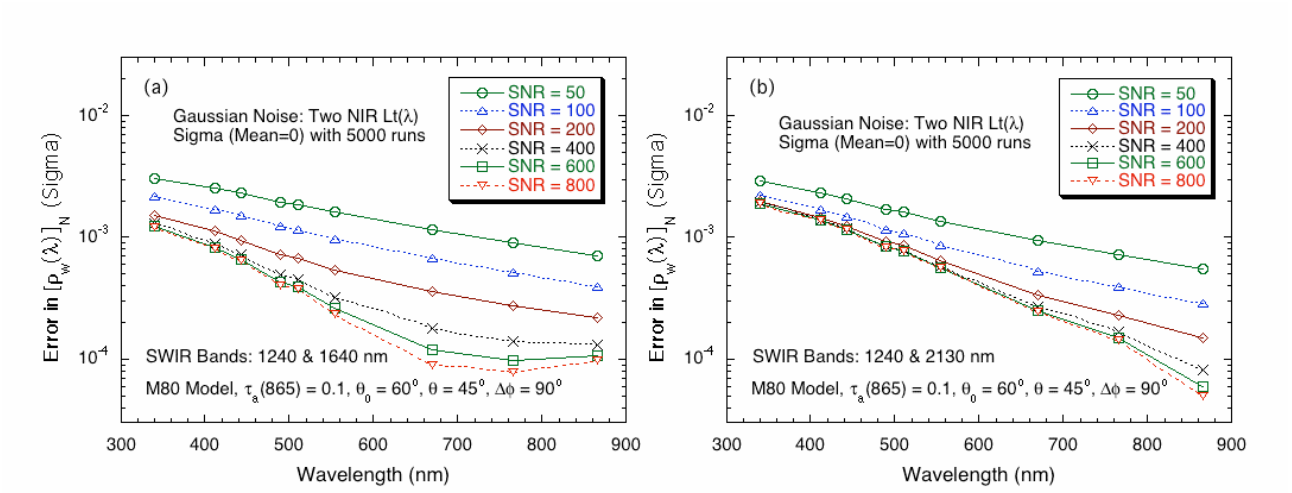

Figure 2. Error in the derived normalized water-leaving reflectance (in standard deviation with the mean value of 0) from 5000 Gaussian noise realizations as a function of the wavelength for various SNR values using the SWIR atmospheric correction algorithm with two SWIR bands of (a) 1240 and 1640 nm and (b) 1240 and 2130 nm. Aerosol model and AOT value, as well as solar-sensor geometry are indicated in each plot.

Example Results. Figure 1 provides sample results in the reflectance uncertainty spectra (UV to red or UV to NIR) with simulations from atmospheric correction algorithm using the NIR or SWIR bands. The error in the normalized water-leaving reflectance, $[\rho_w(\lambda)]_N$, is actually the standard deviation of the derived uncertainty in $[\rho_w(\lambda)]_N$ over the 5000 Gaussian noise realizations, i.e., each point in the plot was derived from 5000 simulations ($[\rho_w(\lambda)]_N$ errors were first obtained with these 5000 simulations and then STD error was derived). The STD error was computed assuming that the mean value = 0 (i.e., error free). Figures 1(a) and 1(b) are results for the NIR atmospheric correction algorithm (using 765 and 865 nm) with the M80 and T80 aerosol models, respectively, while Figures 1(c) and 1(d) are results for the M80 and T80 aerosols using the SWIR atmospheric correction algorithm (with bands of 1240 and 1640 nm) for various SNR values. Note that for the SWIR results (Figures 1(c) and 1(d)), errors in $[\rho_w(\lambda)]_N$ for two NIR bands are also included. Results in Figure 1 show that, as SNR value increases (or noise decreases), error in $[\rho_w(\lambda)]_N$ decreases (as expected), and it reaches the inherent algorithm error (Gordon and Wang, 1994; Wang, 2007).

Figure 2 provides sample results in the reflectance uncertainty spectra as a function of the wavelength (UV to NIR) for various SNR values with simulations from atmospheric correction algorithm using the two SWIR band sets, i.e., 1240 and 1640 nm (Figure 2(a)) and 1240 and 2130 nm (Figure 2(b)). Importantly, results in Figure 2 show that errors in $[\rho_w(\lambda)]_N$ from atmospheric correction are spectrally coherent. In addition, Figure 2 demonstrates that a SNR value between ~200-300 for the SWIR bands 1240 and 1640 nm is adequate (Figure 2(a)), while for the SWIR band 2130 nm a minimum of SNR value ~100 is required. At these SNR values for the SWIR bands, the derived water-leaving reflectance spectra from the SWIR atmospheric correction algorithms almost reach their corresponding algorithm inherent accuracy. It should be

noted that, however, with even higher SNR values the derived $[\rho_w(\lambda)]_N$ at the red and NIR bands can be further improved.

Summary. Atmospheric correction and bio-optical simulations (see results from Stephane Maritorena) suggest that (1) for the NIR bands a minimum SNR value of ~600 is required, and (2) for the SWIR bands at 1240 and 1640 nm a minimum SNR value of ~200-300 is required, while for the 2130 nm band a minimum SNR value of ~100 is adequate.

Bio-optical model sensitivity analysis

Simulations were performed to assess how noise in the spectral marine remote sensing reflectance, Rrs(λ), affects the retrievals of biogeochemical variables from a semi-analytical ocean color model (GSM01, Maritorena et al., 2002). These analyses were performed in order to assess the required SNRs in the ACE visible bands to ensure accurate bio-optical retrievals. Noise is created from the at-sea-level atmosphere reflectance spectra derived from the atmosphere specific simulations ran by Menghua Wang. The spectral atmospheric noise is added to a marine reflectance spectrum at the surface derived from a chlorophyll-based model (Morel and Maritorena, 2001). We compared the model retrievals obtained when spectral reflectance is contaminated by noise to those retrieved from noise-free spectra. These simulations were run for a variety of atmospheric and marine conditions. This is briefly described below.

Two main kinds of noise were considered: 1) Atmospheric noise caused by errors in the NIR bands and propagated to the visible bands and, 2) noise as a random, spectrally uncoherent fraction of the Top-of-Atmosphere (TOA) reflectance in addition to the NIR created noise. This latter case was designed to represent radiometric noise from other sources than the NIR bands (e.g. calibration). These two cases, will be referred to as "NIR" and "radiometric" errors, respectively.

In all runs, the "pure" marine Rrs signal (= no noise) is generated from the MM01 model (Morel & Maritorena, 2001) for 10 chlorophyll concentration (CHL) values in the 0.02-5 mg/m^3 range (400-700 nm every 5 nm). The GSM01 retrievals from the inversion of these "no noise" spectra are the reference to which the "noisy" NIR and radiometric cases are compared to.

For the "NIR" errors case, the at-sea-level reflectance spectra caused by errors in the NIR bands (from Menghua Wang) are converted to Rrs, Rrs_NIR(λ), and added to a MM01 marine spectrum, Rrs_MM01(λ, CHL), so

Rrs(λ, ocean) = Rrs_MM01(λ, CHL)+ Rrs_NIR(λ)

The resulting spectrum, Rrs(λ, ocean), is then inverted in GSM. The three GSM retrievals (CHL, CDM, BBP) are then compared to the "no noise" case for 5000 spectra for each combination of SNR (8 values), AOT(865) and atmospheric model (2 models) and marine Rrs(λ) (10 spectra). The comparisons are expressed in terms of the %rms for each of the GSM01 product and at each Chl level used to generate the marine Rrs. The %rms is defined as rms*100/reference (reference = retrieval in the no noise case).

For the "radiometric" errors case, a random, Gaussian, spectrally uncoherent fraction of a TOA signal is added to the marine spectra created similarly to what is described in the "NIR" case above. First, TOA signals are constructed for a black ocean with the M80 and T80 models, AOT(865) = 0.1 and for solar, sensor, and relative azimuth angles of 60, 45, and 90 degrees, respectively. The ocean contribution to the TOA signal is calculated as a MM01 reflectance spectrum transmitted through the atmosphere (with transmittance values matching the

atmospheric model and geometry and AOT(865) of 0.05, 0.1, 0.2, and 0.3) and is added to the atmospheric TOA component (converted to Rrs units; Rrs_TOA(λ)). The fraction of the TOA signal that is added to the marine spectrum created as in the NIR cases is determined through the generation of random Gaussian numbers with a mean of 0 and a standard-deviation of 1/SNR(visible) with SNR(visible) set to 10., 20., 40., 100., 200., 400., 800., 1000. and 2000. Then, each wavelength of the TOA spectrum is multiplied by a unique random number (rn) and that fraction of the TOA spectrum is added to the other components of the marine signal. This is done independently for each of the 5000 spectra corresponding to each SNR(NIR)/AOT(865)/atmospheric model combination used in the atmosphere simulations. In summary, in the "radiometric" errors case the at-sea-level Rrs is generated as:

Rrs(λ, ocean) = Rrs_MM01(λ, CHL)+ Rrs_NIR(λ) + (Rrs_TOA(λ) * rn(λ, SNR(visible))

By looking at how much the retrievals from the noisy reflectance spectra depart from those derived without addition of noise, it is possible to assess the SNR(visible) value that allows an acceptable accuracy in the retrievals. It should be mentioned that in this approach, we assume an identical SNR level throughout the visible spectrum and does not take into account the fluorescence bands. Figures 3 and 4 illustrate the results of these analyses.

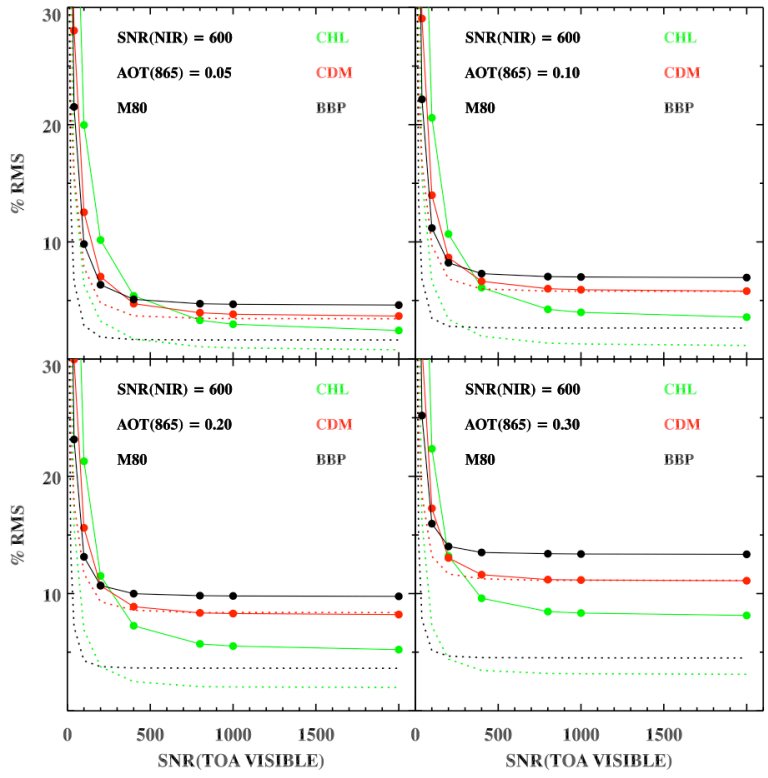

Figure 3. Example of the average (solid lines and symbols) and standard-deviation (dotted lines) of the %rms error over the full range of CHL values used as input in MM01 for the 3 GSM01 retrievals (green: CHL, red: CDM, black: BBP) as a function of the SNR values in the visible and for SNR(NIR)=600 and different AOT(865) values.

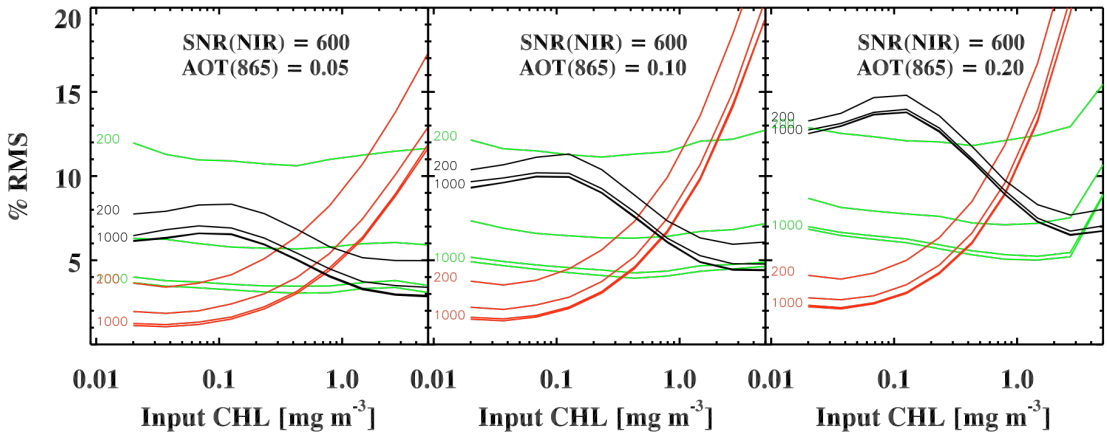

Figure 4. Example of the %rms error for each of the GSM01 retrievals (green: CHL, red: CDM, black: BBP) as a function of the CHL values used as input in MM01 for SNR(NIR)= 600 and different AOT(865) values. For each retrieval, the curves for SNR(visible) of 200, 400, 800 and 1000 are plotted, the highest (=1000) and lowest (=200) SNR(visible) values are indicated at either the beginning or the end of each curve.

For the minimum SNR(NIR) value of 600 suggested above, Figure 4 shows that for the three GSM retrievals the errors become stable in the 800-1000 SNR(vis) range (CHL gets stable at higher SNRs than the other 2 retrievals). The mean error (for the full range of CHL values used as input into MM01) remains under 10% for the clear atmosphere cases only (AOT(865) ≤ 0.1). This is confirmed in Figure 3 where the errors in the GSM retrievals stay under or close to 10% (except for CDM in eutrophic waters) for clear atmospheres and high SNRs. For the visible bands, a minimum SNR of ~1000 is thus recommended.

Measurement requirements summary

The ocean radiometer requirements are outlined in the following two tables. The first provides general sensor performance and mission support requirements. The second lists specific data on multispectral bands, bandwidths, typical clear sky top-of-atmosphere radiances over the ocean, saturation radiances, and minimum SNRs (based on the analyses above). In Table 2, the SNR value at 350 nm is lower than in the other UV bands because its application for detecting absorbing aerosols does not require a value of 1000. Also, the SNR at 678 nm is set at 1400 based on analysis of MODIS retrievals (the bio-optical sensitivity analyses above did not include fluorescence line height). In the wavelength domain of 345-755 nm, multispectral bands are aggregations of 5 nm hyperspectral bands.

Table 1. General requirements for ocean radiometer and mission support.

Radiometer Spectral Attributes

- 26 multispectral bands (Table 2) including
  10 nm fluorescence bands (667, 678, 710, 748 nm band centers)
  10 to 40 nm bandwidth aerosol correction bands at 748, 765, 865, 1245, 1640, 2135 nm
  820 nm band for estimation of column water vapor concentration
  350 nm band for absorbing aerosol detection
- 5 nm resolution 345 to 755 nm (functional group derivative analyses)

- Polarization: < 1.0% sensor radiometric sensitivity, 0.2% prelaunch characterization accuracy
- No saturation in multispectral bands

Accuracy and Stability

- < 2% prelaunch radiance calibration accuracy
- On-orbit vicarious calibration accuracy to 0.2%
- 0.1% radiometric stability knowledge (mission duration)
- 0.1% radiometric stability (1 month prelaunch verification)

Spatial Coverage

- Two day global coverage (58.3^o cross track scanning)
- 1 km resolution at center of swath

Other

- Sensor tilt (±20^o) for glint avoidance
- 5 year minimum design lifetime
- Monthly lunar imaging at 7° phase angle through Earth-view sensor port

λ	∇λ	Ltyp	Lmax	SNR-spec
350	15	7,46	35.6	300
360	15	7.22	37.6	1000
385	15	6.11	38.1	1000
412	15	7.86	60.2	1000
425	15	6.95	58.5	1000
443	15	7.02	66.4	1000
460	15	6.83	72.4	1000
475	15	6.19	72.2	1000
490	15	5.31	68.6	1000
510	15	4.58	66.3	1000
532	15	3.92	65.1	1000
555	15	3.39	64.3	1000
583	15	2.81	62.4	1000
617	15	2.19	58.2	1000
640	10	1.90	56.4	1000
655	15	1.67	53.5	1000
665	10	1.60	53.6	1000
678	10	1.45	51.9	1400
710	15	1.19	48.9	1000
748	10	0.93	44.7	600
765	40	0.83	43.0	600
820	15	0.59	39.3	600
865	40	0.45	33.3	600
1245	20	0.088	15.8	250
1640	40	0.029	8.2	180
2135	50	0.008	2.2	100

Table 2. OES multispectral band centers, bandwidths, typical top-of-atmosphere clear sky ocean radiances (Ltyp), saturation radiances (Lmax), and minimum SNRs at Ltyp. Radiance units are mW/cm^2 μm str.

References

Gordon, H. R. and M. Wang, Retrieval of water-leaving radiance and aerosol optical thickness over the oceans with SeaWiFS: A preliminary algorithm, *Appl. Opt.*, 33, 443-452, 1994.

Maritorena, S., D.A. Siegel and A. Peterson, Optimization of a Semi-Analytical Ocean Color Model for Global Scale Applications. *Applied Optics*. 41:15, 2705-2714, 2002.

Morel A. and S. Maritorena, Bio-optical properties of oceanic waters : a reappraisal. *J. Geophys. Res.*, 106:C4, 7163-7180, 2001.

Wang, M., Remote sensing of the ocean contributions from ultraviolet to near-infrared using the shortwave infrared bands: simulations, *Appl. Opt*., 46, 1535-1547, 2007.